Spin dynamics across metallic layers on the few-femtosecond timescale

Romain Géneaux, Hung-Tzu Chang, Alexander Guggenmos, Renaud Delaunay, François Légaré, Katherine Légaré, Jan Lüning, Tymur Parpiiev, Ilana J. P. Molesky, Bethany R de Roulet, et al.

Spin dynamics across metallic layers at the few-femtosecond timescale

Romain Géneaux,[1,2,3,*] Hung-Tzu Chang,[1,†] Alexander Guggenmos,[1] Renaud Delaunay,[4] François Légaré,[5] Katherine Légaré,[5] Jan Lüning,[6] Tymur Parpiiev,[1] Ilana J.P. Molesky,[1] Bethany R. de Roulet,[1] Michael W. Zuerch,[1,7] Sangeeta Sharma,[8,9] Martin Schultze,[10] and Stephen R. Leone[1,11,12]

[1] *Department of Chemistry, University of California, Berkeley, 94720, USA*
[2] *Université Paris-Saclay, CEA, LIDYL, 91191 Gif-sur-Yvette, France*
[3] *CY Cergy Paris Université, CEA, LIDYL, 91191 Gif-sur-Yvette, France*
[4] *Sorbonne Université, CNRS, Laboratoire de Chimie Physique-Matière et Rayonnement, LCPMR,75005 Paris, France*
[5] *Institut National de la Recherche Scientifique, Centre Énergie Matériaux et Télécommunications, Varennes, Québec, Canada*
[6] *Helmholtz-Zentrum Berlin für Materialien und Energie, Albert-Einstein-Strasse 15, 12489 Berlin, Germany*
[7] *Materials Science Division, Lawrence Berkeley National Laboratory, Berkeley, CA 94720, USA*
[8] *Max-Born-Institute for Non-linear Optics and Short Pulse Spectroscopy, Max-Born Strasse 2A, 12489 Berlin, Germany*
[9] *Institute for Theoretical Solid-State Physics, Freie Universität Berlin, Arnimallee 14, 14195 Berlin, Germany*
[10] *Institute of Experimental Physics, Graz University of Technology, Petersgasse 16, 8010 Graz, Austria*
[11] *Chemical Sciences Division, Lawrence Berkeley National Laboratory, Berkeley, California 94720, USA*
[12] *Department of Physics, University of California, Berkeley, 94720, USA*

We measure the light-driven response of a magnetic multilayer structure made of thin alternating layers of cobalt and platinum at the few-femtosecond timescale. Using attosecond magnetic circular dichroism, we observe how light rearranges the magnetic moment during and after excitation. The results reveal a sub-5 fs spike of magnetization in the platinum layer, which follows the shape of the driving pulse. With the help of time-dependent density functional theory, we interpret the observations as light-driven spin injection across the metallic layers of the structure. The light-triggered spin current is strikingly short, largely outpacing decoherence and dephasing. The findings suggest that the ability of shaping light fields in refined ways could be translated into shaping new forms of spin currents in materials.

In ferromagnetic materials, electrons of opposite spins exhibit different properties. This spin-dependent behavior can create spin-polarized electronic currents – most commonly called spin currents – which are prominent vectors of information [1, 2]. Most remarkably, electron dynamics following femtosecond laser excitation are also spin-dependent, which means that ultrashort laser pulses are able to create spin currents [3], resulting in time-compressed signals that can be transported across complex heterostructures [4]. These techniques allow to store and transport information [5], or to trigger subsequent processes such as terahertz emission [6, 7].

However, our abilities to create spin currents with laser pulses are still limited. To date, the spin-polarization of electrons arises from incoherent mechanisms. For instance, majority carriers may experience longer mean free paths [3, 8] or longer lifetime following optical excitation [9], which allows to selectively inject them into other materials. While this provides efficient spin injection, the incoherent nature of scattering means that the temporal shape of the created spin currents are set by inherent material properties, and not by the temporal structure of the driving laser pulse. As a result, it is hitherto unclear how to coherently control magnetic properties at femtosecond timescales, or to drive spin dynamics at optical frequencies.

Here we show that spin currents can actually be created at extremely short times – before incoherent processes start to play a role. One hint that it is indeed possible was obtained in earlier works [10, 11] and particularly in a recent breakthrough [12], which showed that the magnetization of ferromagnetic layer reacted instantaneously to a laser-field, when put in contact with a Pt layer. Interpretation of these observations hypothesized the rapid onset of an interface spin current created by a mechanism called optical inter-site spin transfer (OISTR [13]), which we set out to explore here. Our strategy relies on driving ferromagnetic/paramagnetic heterostructures with few-cycle pulses, and to probe spin injection across the structure using attosecond metrology. We investigate spin dynamics in a multilayer sample of Co/Pt, containing 20 periods of cobalt and platinum interfaces, each layer being 6 and 8 Å thick, respectively (see Fig. 1a). This type of structure is ubiquitous in spintronic research, in particular to obtain giant magnetoresistance effects [14, 15]. This particular layer arrangement has two advantages for our purposes: (i) it creates an out-of-plane magnetic easy axis [16], maximizing magneto-optical effects with normally incident light; (ii) it multiplies the number of Co/Pt interfaces, so that potential injection taking place there becomes more measurable compared to bulk regions. The sample is placed in an external out-of-plane magnetic field, saturating the magnetization of the ferromagnetic Co layers as well as weakly magnetizing the Pt layers by proximity effects, even though the latter are paramagnetic [17, 18]. The sample is capped on both sides to prevent oxidation.

To resolve eventual spin transfer phenomena, we lever-

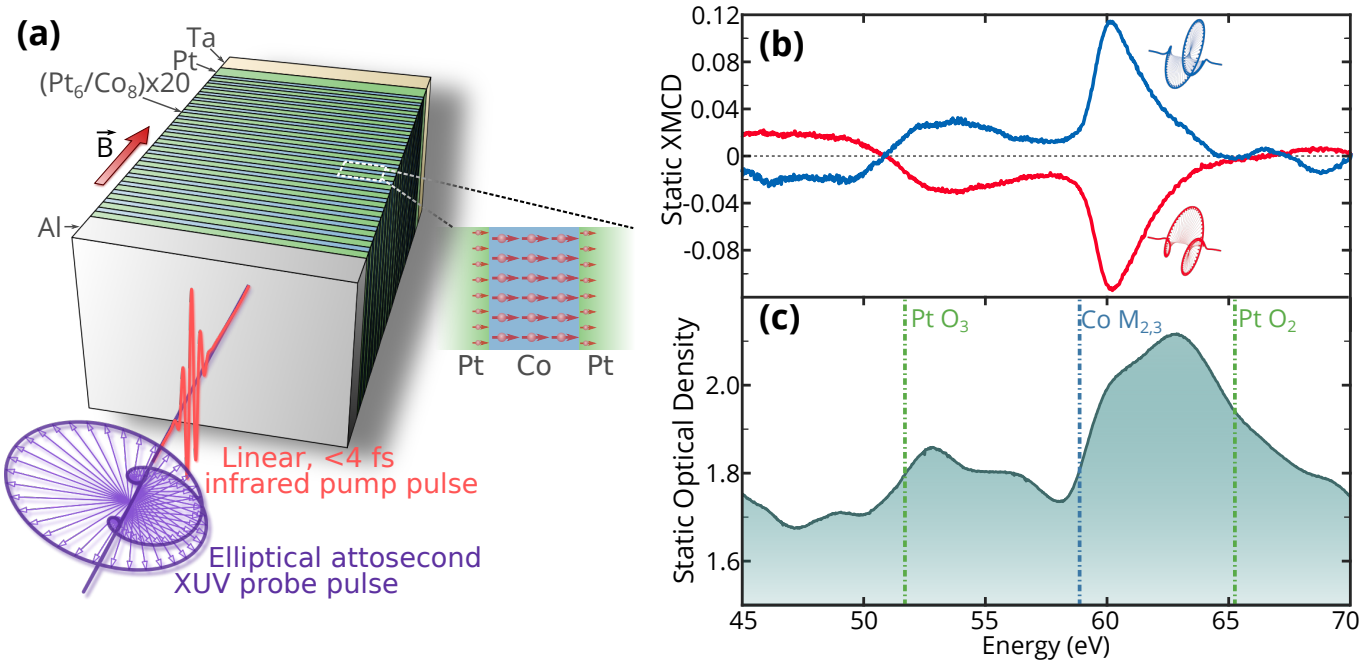

FIG. 1. **Schematic of the experiment and static characterization. a.** Co/Pt multilayer sample used in the experiment. It consists of 20 periods, and is capped on both sides to prevent oxidation. The inset shows that in an external magnetic field, both Co and Pt layers are magnetized **b.** Static XMCD measured with positive or negative XUV helicity (blue and red lines, respectively). **c.** Static optical density (without excitation) across the attosecond pulse bandwidth. Green and blue vertical lines indicate the Pt and Co absorption edges, respectively.

age the element-sensitivity of core-level spectroscopy, together with the outstanding time resolution of attosecond spectroscopy. We measure the sample absorption using broadband XUV attosecond pulses covering 40-70 eV. Figure 1c displays the static optical density of the sample in this spectral region, in which absorptions from both the Co 4p and Pt 6p core-levels are visible, corresponding to the Co $M_{2,3}$ and O_3 edges. O_3-edge attosecond spectroscopy has recently been demonstrated in several elements [19–21]. To add spin resolution, the polarization of the attosecond pulses is set to elliptical by specialized XUV optics (Ultrafast Innovations). This allows measuring the XUV Magnetic Circular Dichroism (XMCD), defined as XMCD $= \log I_+/I_-$, where $I_\pm$ corresponds to the recorded transmission with the sample magnetized along or oppositely from the laser propagation axis, respectively. Figure 1b shows the static XMCD for the two helicities of incoming XUV radiation, displaying a nice mirroring. Compared to literature values, the amplitude of the peaks is reduced by the ellipticity of the XUV pulse (60% on average in the probed energy range), but their shape matches well: the larger peak around 60 eV is the $M_{2,3}$ XMCD of pure cobalt [22] and the broader peak at 51-56 eV corresponds to the Pt O_3 edge [23]. These two features will be used to analyze the respective spin dynamics of each element.

The sample is then excited by a sub-4 fs visible/near-infrared laser pulse, with linear polarization. The change in optical density is measured successively when magnetizing the sample along or opposed to the laser propagation direction, yielding ΔOD_{B_+} and ΔOD_{B_-} (shown separately in the Supplemental Material [24]). Figure 2a shows the purely electronic response, isolated by taking $\Delta OD = (\Delta OD_{B_+} + \Delta OD_{B_-})/2$. As soon as the sample is excited (delay $t > 0$), changes are measured across the entire probed spectral range. The strongest features are red shifts of both Pt and Co edges (lineouts are shown in SM [24]), similar to the behavior of laser-heated nickel described in great detail in earlier work [25]. The magnetic response is quantified through the change in XMCD: $\Delta\text{XMCD} = \Delta OD_{B_+} - \Delta OD_{B_-}$, shown in Figure 2b. Reversing the helicity of the XUV light results in a sign change of the entire measurement (see SM [24]), confirming that all observed features originate from a real dichroic response. In this 200 fs-long trace, we can readily see that the overall trend is mostly a decrease of the magnitude of the dichroism at all energies, consistent with femtosecond demagnetization of the sample at a slow timescale. To our knowledge, this is the first time that time-resolved XMCD is measured over such a broad and continuous energy range, covering core transitions of both elements of the heterostructure. Since the probe light spectrum is continuous, we measure not only changes of amplitudes at specific discrete energies, but also any change in the spectral shape of magnetic dichroism. This ability was also demonstrated in a recent study

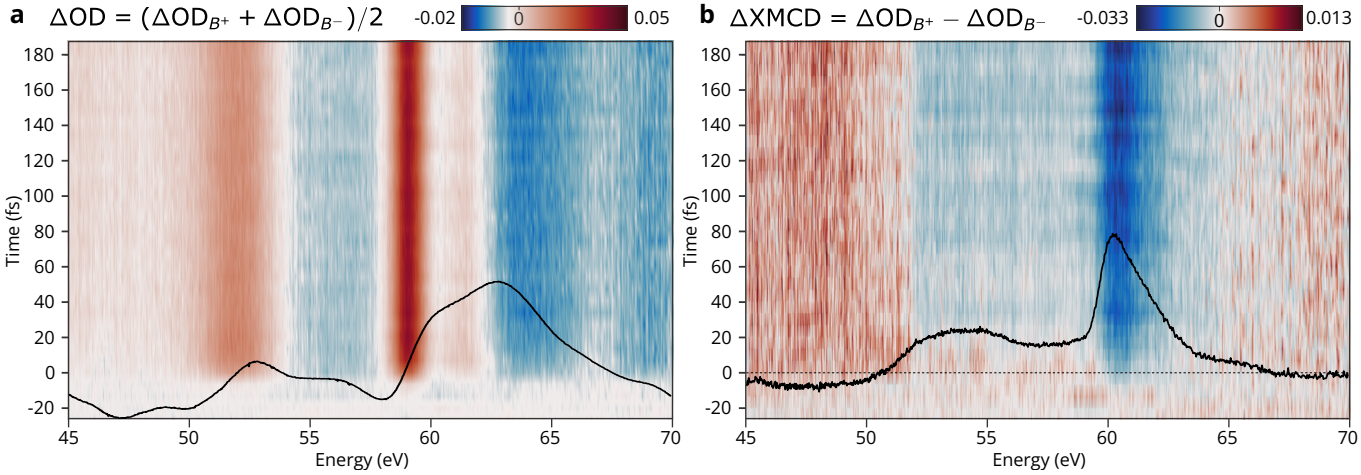

FIG. 2. **Time-dependent XUV magnetic circular dichroism. a.** Change in optical density obtained by averaging the measurements for each magnetization direction. The overlaid black line is the static optical density. The experimental excitation fluence is 25 ± 2 mJ/cm^2 and the pump pulse duration is 3.5 ± 0.4 fs. **b.** Change in XUV magnetic circular dichroism, obtained by subtracting the two optical density maps. The black line is the static XMCD of the sample.

on Heusler alloys [26]. Distinguishing between lineshape or amplitude changes is a known hindrance when using narrowband light, such as discrete HHG sources, most free-electron lasers and synchrotron radiation [27]. Moreover, because the entire XMCD is captured at once, the approach is particularly time-efficient. Thus, the method should be advantageous to probe magnetic dynamics at any timescale.

We focus on the few femtoseconds timescale, which is experimentally attainable here, contrary to the majority of previous experiments. To this end, we perform finer transient XMCD scans with time steps of 333 as. We first consider the electronic dynamics obtained by averaging the two sample magnetizations. Following previously established methodology for XUV transient absorption in pure transition metals [25], we integrate the prominent positive signal right below the absorption edges (around 52 eV for Pt and 59 for Co) to quantify the edge shifts, and show the resulting signal rise in Fig. 3(a). We find that the electronic charges respond simultaneously in Co and Pt within an uncertainty of 1.5 fs, which is in line with previous attosecond measurements in metals [12, 25, 28]. However, in all measurements including the one shown here, the Pt signal rises 1.5 times faster than in Co. One possibility for this disparity is that each element has different electron-electron thermalization times [25, 29]. However, we found that the same measurement performed in elemental Co and Pt clearly showed the opposite trend, with electrons in Co thermalizing faster than in Pt [30]. Thus we conclude that the disparity must be specific to the heterostructure and thus rooted in charge flow across the interfaces.

To now gain insight into the response of the spin system, the transient XMCD trace needs to be converted into physically meaningful parameters for each layer. At each time delay, we have [23]:

$$\mathrm{XMCD}(t,\omega) = -\frac{4d_{Pt}\omega}{cP}\beta_{Pt}(t,\omega) - \frac{4d_{Co}\omega}{cP}\beta_{Co}(t,\omega), \quad (1)$$

where $d_{Pt/Co}$ are the total thicknesses and $\beta_{Pt/Co}$ the imaginary part of the magneto-optical function of each element, c the speed of light, P the degree of circular polarization and w the photon frequency. The broadband measurement shows that none of the observed peaks are spectrally shifting, nor are they changing shape (see SM [24]). Therefore we consider that the magneto-optical functions of Pt and Co are not changing shape as a function of time, a possibility that was raised in Ref. [27]. Thus we write the time dependence of β_{Pt} and β_{Co} as a time-varying scaling coefficient, $a_{Pt/Co}(t)$, meaning the XMCD is a linear combination of two spectral components corresponding to the two elements:

$$\mathrm{XMCD}(t) \propto d_{Pt}a_{Pt}(t)\cdot\beta_{Pt}(\omega) + d_{Co}a_{Co}(t)\cdot\beta_{Co}(\omega), \quad (2)$$

where $\beta_{Pt/Co}$ are taken as their ground-state values known from synchrotron measurements [22]. The time-dependent amplitudes obtained by fitting the change in XMCD are displayed in Figure 3(b) and represent the change in magnetic moment in each layer [23]. Here, attosecond spectroscopy brings a key advantage: we distinguish magnetic dynamics taking place during or after the pump pulse. This uncovers a striking behavior: during excitation (highlighted area in Fig. 3(b)), the cobalt magnetization is quenched at a very high rate, with the magnetic moment being already suppressed by 10% only 2 fs after the peak of the pump pulse. At the same time, the platinum magnetic moment shows a clear increase of a few percent. Once the pump pulse has passed, the sample follows a more conventional field-free behavior: both

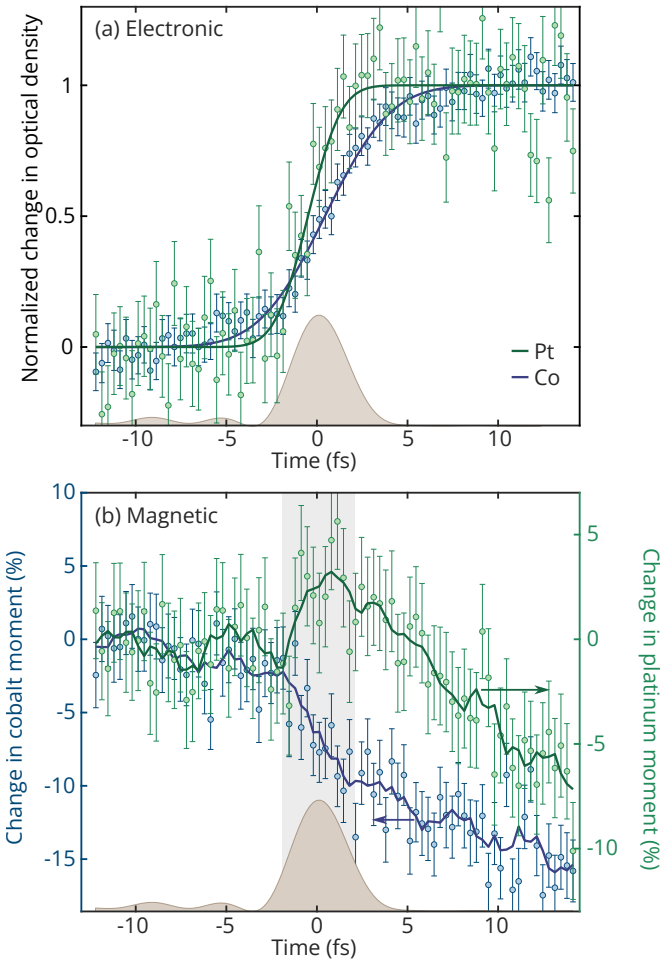

FIG. 3. **Electronic and magnetic dynamics at the few-femtosecond timescale a.** Normalized change in optical density at the Co (blue) and Pt (green) edges. Dots are data points, with error bars the standard deviation of several measurement for each time delay. Full lines are exponential fits of the response. **b.** Change in magnetic moment expressed in percent of the ground-state value for Co (blue) and Pt (green). Circles are data points, with error bars obtained by Monte Carlo propagation of uncertainties. Full lines show a moving average of data points. In both panels, the brown shaded area is the experimental pump intensity profile obtained by a dispersion-scan measurement.

layers begin to demagnetize on timescales in correspondence with literature reports on laser induced demagnetization. Measurements at longer times (shown in SM [24]) show that the maximum quenching is attained at $t = 150$ fs and amounts to 30% for Co and 20% for Pt, compared to their equilibrium value.

The observed behavior strongly suggests that the laser pulse triggers a net transfer of charge and spin from cobalt layers into platinum, consistently with the OISTR mechanism [13]. To confirm this, we turn to state-of-the-art time-dependent density functional theory (TDDFT), which has been very successful at calculating magnetic dynamics at short times [10, 12, 13, 23]. The computational cost of such calculations limits us to simulating only a few atomic layers. Therefore, we consider an $L1_0$-ordered 50-50 alloy of CoPt, which reproduces well the Co/Pt interface of our sample at the atomic level. This model will not be able to reproduce any bulk effect in individual layers, nor an effect due to the periodic multilayer structure of the real sample. However, the physics of such thin layers are known to be dominated by interface effects [31] and as such should be reasonably reproduced by the theory. We use the highly accurate full potential linearized augmented-plane-wave method, as implemented in the ELK code [32]. For time propagation we used a time step of 2 attoseconds and the algorithm outlined in Ref. [33]. More details are available in the SM [24]. Figure 4(a) displays the obtained relative change in magnetic moment for each element, with a pump intensity of $2 \times 10^{11}\,\mathrm{W\,cm^{-2}}$. The calculation reproduces well the behavior observed experimentally during the pump pulse. The magnetic moment of Co and Pt are decreasing and increasing, respectively, with a shape that closely follows $\beta(t) \propto \int_{-\infty}^{t} I_{\mathrm{pump}}(\tau)d\tau$, which is consistent with the phenomenon being driven by electronic injection. We also calculate the relative change in XMCD for the Co $M_{2,3}$ and Pt O_3 edges at a few time delays, shown as crosses in Fig. 4(a). We find that the XMCD amplitudes follow the dynamics of the local spin moments in each element, confirming the validity of the experimental data analysis. However, the calculation overestimates the change of Pt moment, compared to the experiment. This is most likely because the computation does not include any incoherent interaction, such as scattering with phonons or spin diffusion, which are additional channels for demagnetization. Additionally, the many Co/Pt interfaces present in the experiment are imperfect, and the measurement averages the signal over all of them. These factors can result in an overall reduction of the measured Pt moment. The calculations also display fast oscillations of the magnetic moments at twice the laser field period, which are inaccessible to the experiment due to insufficient sensitivity. We note that these oscillations could be spurious effects from the calculation, which does not include dissipation channels.

Both experiment (Fig. 3(b)) and theory (Fig. 4(a)) are consistent with OISTR with a net spin transfer from Co to Pt, accompanying majority carriers from Co to Pt and minority carriers from Pt to Co. The mechanism is also compatible with the faster electronic excitation observed in Pt(Fig. 3(a)): as the laser injects Co majority spins into Pt, it leads to more excited carriers in Pt layers at early times. Most importantly, at timescales considered here, spin injection is not mediated by incoherent effects. Instead, it is made possible by the favorable band alignment at the Co/Pt interface, as already noticed in Ref. [13]. Although dichroism measurements do not directly probe currents, the concomitant change in

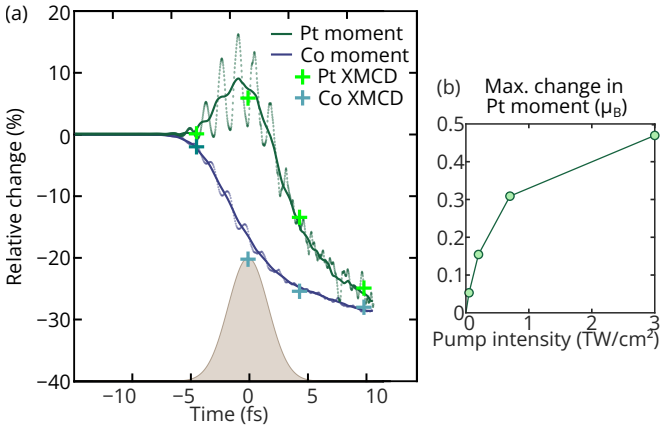

FIG. 4. **Ab initio simulations of magnetic dynamics a.** Computed change in magnetic moment expressed in percent of the ground-state value for Co (blue) and Pt (green). Dots are raw data points, full lines are a moving average and crosses are computed integrated XMCD for specific time delays. The brown shaded area is the pump intensity profile used in the calculation. **b.** Maximum change in platinum moment expressed in units of μ_B computed for varying pump intensities.

magnetic moments of both layers indicates a spin current which stands out due to its extremely short, few femtosecond duration. Finally, we computationally explored the intensity dependence of the effect. Figure 4(b) shows the maximum Pt moment as a function of pumping intensity. The dependence is found to be sub-linear, and the spin injection seems to take place even at lower intensities. Experimentally, we only observed spin injection with very short pulses, most likely because overcoming the experimental noise floor required sufficient intensity, while staying below the sample damage threshold. But the calculations suggest that the effect is more universal and could be observed for longer or less intense driving pulses.

In summary, we investigated the electronic and magnetic dynamics of a Co/Pt multilayer structure at the few-femtosecond timescale. While spin responses on such timescale have been reported before [10–12], our work provides new information mainly because of the ability to directly capture charge and spin dynamics simultaneously for both elements. As a result, we uncover a direct observation of laser-induced spin injection between metallic layers. This effect takes place in synchrony with the laser envelope, which is a key difference with other types of light-triggered spin dynamics, such as the ones responsible for terahertz emission [6]. This opens the way to the possibility of shaping the envelope of laser pulses to manipulate the magnetization in time, which can eventually lead to the enhancement and control of spin currents. The dynamics measured here can be seen as the first example of such shaping: by using temporally compressed driving pulses, we create a spin current lasting only a few femtoseconds, which is the shortest spin current observed to date.

Generally, we show that attosecond methodology answers two questions that are key for fundamental understanding and potential applications of spintronic devices at ultrafast timescales: it captures how ultrashort spin-polarized currents can be created and how they are injected across materials. We believe that it is not only this specific multilayer structure that can display ultrashort spin currents – any spintronic structure with proper band alignement between its layers might do the same. With ever-increasing sensitivity in attosecond metrology, light-induced manipulation of magnetization could even evolve from envelope-driven effects, such as captured here, to coherent field-driven effects, as initially formulated by Bigot et al. [34]. While our experiment had insufficient sensitivity to capture them, future attosecond technology will surely allow to tackle these fascinating questions.

Investigations at UC Berkeley were supported by the U.S. Air Force Office of Scientific Research Nos. FA9550-19-1-0314 (primary), FA9550-20-1-0334, FA9550-22-1-0451, FA9550-15-0037 (concluded), and FA9550-14-1-0154 (concluded), the Defense Advanced Research Projects Agency PULSE Program Grant W31P4Q-13-1-0017 (concluded), and the W.M. Keck Foundation award No. 046300-002 (concluded). R.G. acknowledges funding by the European Union (ERC Spinfield, Project No. 101041074). H.T.C acknowledges funding from the Alexander von Humboldt Foundation. K.L. acknowledges support from the NSERC Alexander Graham Bell Canada Graduate Scholarships program. Sharma would like to thank the DFG for funding through project-ID 328545488 TRR227 (project A04) and Leibniz Professorin Program (SAW P118/2021).

* romain.geneaux@cea.fr
† Current address: Max Planck Institute for Multidisciplinary Sciences, 37077 Goettingen, Germany

[1] G. Binasch, P. Grünberg, F. Saurenbach, and W. Zinn, Enhanced magnetoresistance in layered magnetic structures with antiferromagnetic interlayer exchange, Physical Review B **39**, 4828 (1989).
[2] M. N. Baibich, J. M. Broto, A. Fert, F. N. Van Dau, F. Petroff, P. Etienne, G. Creuzet, A. Friederich, and J. Chazelas, Giant Magnetoresistance of (001)Fe/(001)Cr Magnetic Superlattices, Physical Review Letters **61**, 2472 (1988).
[3] M. Battiato, K. Carva, and P. M. Oppeneer, Superdiffusive Spin Transport as a Mechanism of Ultrafast Demagnetization, Physical Review Letters **105**, 027203 (2010).
[4] I. Žutić, J. Fabian, and S. Das Sarma, Spintronics: Fundamentals and applications, Reviews of Modern Physics **76**, 323 (2004).

[5] A. Brataas, A. D. Kent, and H. Ohno, Current-induced torques in magnetic materials, Nature Materials **11**, 372 (2012).

[6] T. Seifert, S. Jaiswal, U. Martens, J. Hannegan, L. Braun, P. Maldonado, F. Freimuth, A. Kronenberg, J. Henrizi, I. Radu, E. Beaurepaire, Y. Mokrousov, P. M. Oppeneer, M. Jourdan, G. Jakob, D. Turchinovich, L. M. Hayden, M. Wolf, M. Münzenberg, M. Kläui, and T. Kampfrath, Efficient metallic spintronic emitters of ultrabroadband terahertz radiation, Nature Photonics **10**, 483 (2016).

[7] D. Yang, J. Liang, C. Zhou, L. Sun, R. Zheng, S. Luo, Y. Wu, and J. Qi, Powerful and Tunable THz Emitters Based on the Fe/Pt Magnetic Heterostructure, Advanced Optical Materials **4**, 1944 (2016).

[8] A. Eschenlohr, M. Battiato, P. Maldonado, N. Pontius, T. Kachel, K. Holldack, R. Mitzner, A. Föhlisch, P. M. Oppeneer, and C. Stamm, Ultrafast spin transport as key to femtosecond demagnetization, Nature Materials **12**, 332 (2013).

[9] L. Cheng, X. Wang, W. Yang, J. Chai, M. Yang, M. Chen, Y. Wu, X. Chen, D. Chi, K. E. J. Goh, J.-X. Zhu, H. Sun, S. Wang, J. C. W. Song, M. Battiato, H. Yang, and E. E. M. Chia, Far out-of-equilibrium spin populations trigger giant spin injection into atomically thin MoS2, Nature Physics **15**, 347 (2019).

[10] F. Willems, C. von Korff Schmising, C. Strüber, D. Schick, D. W. Engel, J. K. Dewhurst, P. Elliott, S. Sharma, and S. Eisebitt, Optical inter-site spin transfer probed by energy and spin-resolved transient absorption spectroscopy, Nature Communications **11**, 871 (2020).

[11] P. Tengdin, C. Gentry, A. Blonsky, D. Zusin, M. Gerrity, L. Hellbrück, M. Hofherr, J. Shaw, Y. Kvashnin, E. K. Delczeg-Czirjak, M. Arora, H. Nembach, T. J. Silva, S. Mathias, M. Aeschlimann, H. C. Kapteyn, D. Thonig, K. Koumpouras, O. Eriksson, and M. M. Murnane, Direct light-induced spin transfer between different elements in a spintronic Heusler material via femtosecond laser excitation., Science advances **6** (2020).

[12] F. Siegrist, J. A. Gessner, M. Ossiander, C. Denker, Y.-P. Chang, M. C. Schröder, A. Guggenmos, Y. Cui, J. Walowski, U. Martens, J. K. Dewhurst, U. Kleineberg, M. Münzenberg, S. Sharma, and M. Schultze, Light-wave dynamic control of magnetism, Nature **571**, 240 (2019).

[13] J. K. Dewhurst, P. Elliott, S. Shallcross, E. K. U. Gross, and S. Sharma, Laser-Induced Intersite Spin Transfer, Nano Letters **18**, 1842 (2018).

[14] F. Garcia, F. Fettar, S. Auffret, B. Rodmacq, and B. Dieny, Exchange-biased spin valves with perpendicular magnetic anisotropy based on (Co/Pt) multilayers, Journal of Applied Physics **93**, 8397 (2003).

[15] S. Mangin, D. Ravelosona, J. A. Katine, M. J. Carey, B. D. Terris, and E. E. Fullerton, Current-induced magnetization reversal in nanopillars with perpendicular anisotropy, Nature Materials **5**, 210 (2006).

[16] P. F. Carcia, Perpendicular magnetic anisotropy in Pd/Co and Pt/Co thin-film layered structures, Journal of Applied Physics **63**, 5066 (1988).

[17] M. Suzuki, H. Muraoka, Y. Inaba, H. Miyagawa, N. Kawamura, T. Shimatsu, H. Maruyama, N. Ishimatsu, Y. Isohama, and Y. Sonobe, Depth profile of spin and orbital magnetic moments in a subnanometer Pt film on Co, Physical Review B **72**, 054430 (2005).

[18] R. M. Rowan-Robinson, A. A. Stashkevich, Y. Roussigné, M. Belmeguenai, S.-M. Chérif, A. Thiaville, T. P. A. Hase, A. T. Hindmarch, and D. Atkinson, The interfacial nature of proximity-induced magnetism and the Dzyaloshinskii-Moriya interaction at the Pt/Co interface, Scientific Reports **7**, 16835 (2017).

[19] H.-T. Chang, A. Guggenmos, C. T. Chen, J. Oh, R. Géneaux, Y.-D. Chuang, A. M. Schwartzberg, S. Aloni, D. M. Neumark, and S. R. Leone, Coupled valence carrier and core-exciton dynamics in WS_2 probed by few-femtosecond extreme ultraviolet transient absorption spectroscopy, Physical Review B **104**, 064309 (2021).

[20] C. A. Leahy and J. Vura-Weis, Femtosecond Extreme Ultraviolet Spectroscopy of an Iridium Photocatalyst Reveals Oxidation State and Ligand Field Specific Dynamics, The Journal of Physical Chemistry A **126**, 9510 (2022).

[21] E. W. de Vos, S. Neb, A. Niedermayr, F. Burri, M. Hollm, L. Gallmann, and U. Keller, Ultrafast Transition from State-Blocking Dynamics to Electron Localization in Transition Metal β-Tungsten, Physical Review Letters **131**, 226901 (2023).

[22] F. Willems, S. Sharma, C. v. Korff Schmising, J. K. Dewhurst, L. Salemi, D. Schick, P. Hessing, C. Strüber, W. D. Engel, and S. Eisebitt, Magneto-Optical Functions at the 3p Resonances of Fe, Co, and Ni: Ab initio Description and Experiment, Physical Review Letters **122**, 217202 (2019).

[23] J. K. Dewhurst, F. Willems, P. Elliott, Q. Z. Li, C. V. K. Schmising, C. Strüber, D. W. Engel, S. Eisebitt, and S. Sharma, Element Specificity of Transient Extreme Ultraviolet Magnetic Dichroism, Physical Review Letters **124**, 077203 (2020).

[24] See Supplemental Material at [url] for theoretical methods, additional measurements with the other XUV helicity, lineouts of XMCD as a function of time and magnetic dynamics at longer timescales, which includes Refs. [35, 36].

[25] H.-T. Chang, A. Guggenmos, S. K. Cushing, Y. Cui, N. U. Din, S. R. Acharya, I. J. Porter, U. Kleineberg, V. Turkowski, T. S. Rahman, D. M. Neumark, and S. R. Leone, Electron thermalization and relaxation in laser-heated nickel by few-femtosecond core-level transient absorption spectroscopy, Physical Review B **103**, 064305 (2021).

[26] S. A. Ryan, P. C. Johnsen, M. F. Elhanoty, A. Grafov, N. Li, A. Delin, A. Markou, E. Lesne, C. Felser, O. Eriksson, H. C. Kapteyn, O. Grånäs, and M. M. Murnane, Optically controlling the competition between spin flips and intersite spin transfer in a Heusler half-metal on sub-100-fs time scales, Science Advances **9** (2023).

[27] K. Yao, F. Willems, C. von Korff Schmising, I. Radu, C. Strüber, D. Schick, D. Engel, A. Tsukamoto, J. K. Dewhurst, S. Sharma, and S. Eisebitt, Distinct spectral response in M-edge magnetic circular dichroism, Physical Review B **102**, 100405 (2020).

[28] M. Volkov, S. A. Sato, F. Schlaepfer, L. Kasmi, N. Hartmann, M. Lucchini, L. Gallmann, A. Rubio, and U. Keller, Attosecond screening dynamics mediated by electron localization in transition metals, Nature Physics **15**, 1145 (2019).

[29] B. Y. Mueller and B. Rethfeld, Relaxation dynamics in laser-excited metals under nonequilibrium conditions, Physical Review B **87**, 035139 (2013).

[30] B. R. de Roulet, L. Drescher, S. A. Sato, and S. R.

Leone, Initial electron thermalization in metals measured by attosecond transient absorption spectroscopy, arXiv:2406.03567 (2024).
[31] K. Krieger, P. Elliott, T. Müller, N. Singh, J. K. Dewhurst, E. K. U. Gross, and S. Sharma, Ultrafast demagnetization in bulk versus thin films: an ab initio study, Journal of Physics: Condensed Matter **29**, 224001 (2017).
[32] J. K. Dewhurst, S. Sharma, L. Nordström, F. Cricchio, O. Grånäs, and E. K. U. Gross, The ELK code.
[33] J. Dewhurst, K. Krieger, S. Sharma, and E. Gross, An efficient algorithm for time propagation as applied to linearized augmented plane wave method, Computer Physics Communications **209**, 92 (2016).
[34] J.-Y. Bigot, M. Vomir, and E. Beaurepaire, Coherent ultrafast magnetism induced by femtosecond laser pulses, Nature Physics **5**, 515 (2009).
[35] E. Runge and E. K. U. Gross, Density-Functional Theory for Time-Dependent Systems, Physical Review Letters **52**, 997 (1984).
[36] U. v. Barth and L. Hedin, A local exchange-correlation potential for the spin polarized case. i, Journal of Physics C: Solid State Physics **5**, 1629 (1972).